Chemical Engineering Journal 149 (2009) 143–152

Contents lists available at ScienceDirect

Chemical Engineering Journal

journal homepage: www.elsevier.com/locate/cej

Long-term performance of zeolite Na A-X blend as backfill material in near surface disposal vault

R.O. Abdel Rahman [a,*], H.A. Ibrahim [a], N.M. Abdel Monem [b]

[a] Hot Laboratory Center, Atomic Energy Authority of Egypt, P.O. 13759, Inshas, Cairo, Egypt
[b] Chemical Engineering Department, Faculty of Engineering, Cairo University, Egypt

ARTICLE INFO

Article history:
Received 28 June 2008
Received in revised form 6 October 2008
Accepted 9 October 2008

Keywords:
Radioactive wastes
Backfill material
Synthetic zeolite
Mathematical models

ABSTRACT

This study investigates the feasibility of using synthetic zeolite Na A-X blend prepared from fly ash as near surface disposal backfill material. Tests were conducted at laboratory scale to evaluate the physical and chemical properties of the prepared zeolite. The zeolite density, porosity, and particle size distribution were measured. The distribution coefficient (K_d) value of Cs ions was evaluated using batch sorption experiment in synthetic groundwater to simulate possible conditions for near surface disposal. The transient behavior of the batch sorption experimental data were analyzed using Lagergren, Ho and Mckay, and Morris–Weber rate models to assess the controlling mechanism of the sorption process. It was found that the sorption process is chemisorption and controlled by diffusion mechanism. The dispersional behavior of Cs ions on the prepared material was studied using column experiment and the hydrodynamic dispersion coefficient was determined. To provide an overall functional performance of the proposed backfill material, the long-term behavior of the prepared zeolite has been evaluated using computer model. This model consists of two modules that has been developed to study the migration of Cs radionuclides from bare cementitious waste form through the backfill. The study compares the release rate from bentonite–crushed rock mixture to that from the prepared zeolite. The result demonstrates that synthetic zeolite Na A-X blend shows a better performance in terms of radionuclide containment.

© 2008 Elsevier B.V. All rights reserved.

1. Introduction

Near surface disposal of low- and intermediate-level radioactive wastes (LILRW) is intended to isolate these wastes from the accessible environment during a period sufficiently long to allow substantial decay of the shorter lived radionuclides and, in the longer term, to limit releases of the remaining radionuclides. To achieve this aim, the multi-barrier concept that relay on engineered barriers to augment natural barriers has been developed. The use of engineered barriers helps in ensuring that increasingly stringent design aims are satisfied to an appropriate level [1]. This concept helps in avoiding over-reliance on one component of the disposal system (i.e. natural barriers) to provide the necessary safety and allow for certain component to fail without compromising the overall safety of the disposal system [2].

Engineered barriers may consist of a number of separate components, including structural walls, buffer or backfill materials, chemical additives, liners, covers, leachate collection and drainage systems, cut-off walls, gas vents and monitoring wells [3]. Buffer or backfill materials surround the waste packages in their emplacement at the disposal facility. Their principle functions are to provide structural stability of the disposal units, reduce the potential for subsidence, minimize the transport of radionuclides released from failed waste packages, and to limit the access of any infiltrating water to the waste packages [4–6].

Different backfill materials have been suggested, notably cement grouts, sand, bentonite, rock, gravel, and compacted clays [5–10]. Bentonite–sand and bentonite–crushed rock mixtures are commonly used in nuclear waste repositories due to their high-erosion resistance, and their mechanical and chemical stability [11–14]. Research has been undertaken concerning evaluation of physical, chemical, hydraulic, thermal, and mechanical properties for different backfill materials [15–22]. Compacted clays, especially those containing appreciable amount of bentonite, have shown problems with shrinkage and or desiccation cracking [17,23–27]. On the other hand, zeolites has been suggested as alternative material because of its high-cation exchange capacity and mechanical stability [28,29].

Hot Laboratory and Waste Management Center (HLWMC) established a research program to synthesize zeolite from fly ash. The aim of this program is to solve the disposal problem of fly ash by utilizing

* Corresponding author. Tel.: +20 16 1404462; fax: +20 2 462 0796.
E-mail addresses: karimrehab1@yahoo.com, alaarehab@yahoo.com (R.O. Abdel Rahman).

1385-8947/$ – see front matter © 2008 Elsevier B.V. All rights reserved.
doi:10.1016/j.cej.2008.10.011

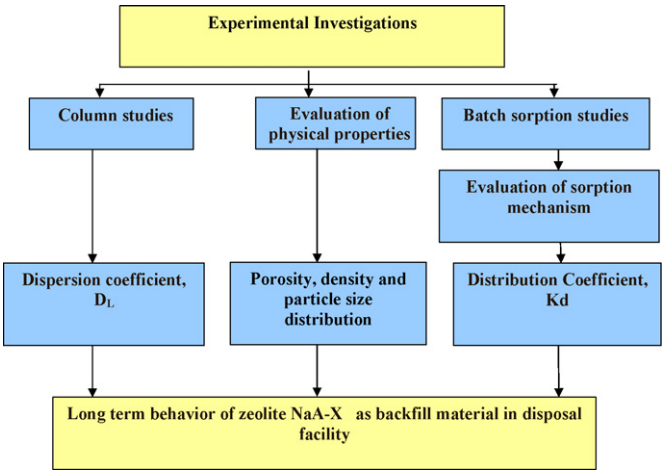

Fig. 1. Flowchart of the work procedure.

it in the production of synthetic zeolite. So that this productive use of fly ash would have environmental benefits, i.e. reduce air, water and soil contamination. This study is a continuation of our previous work [30], at which zeolite Na A-X blend was synthesized, characterized, and its sorption behavior was evaluated. In this paper, the results of detailed investigations of the Cs retention and transport through the proposed backfill material are presented. The laboratory observations of batch and column experiments are analyzed, and the long-term performance of this material is addressed by conducting a quantitative prediction of Cs migration using numerical modeling, the flowchart of the utilized procedure is illustrated in Fig. 1.

2. Experimental

2.1. Chemical and reagents

Fly ash used in this study was produced from thermal electrical power station. Sodium aluminates and sodium hydroxide were used as aluminum and sodium sources to prepare the zeolite blend. To simulate the geochemical conditions in disposal facility, the aqueous phase used for the batch sorption and column experiments were synthetic compositions of groundwater (Table 1) [31]. Then the stable carrier solution was prepared to have 50 mg/l of CsCl.

Table 1
Chemical composition of synthetic groundwater.

Composition	wt%
CaO	63
SiO_2	20
Al_2O_3	6
Fe_2O_3	3
MgO	1.5
SiO_3	2
Na_2O	0.5
K_2O	0.5
Others	0.5
pH	6.5

2.2. Preparation of zeolite Na A-X blend

A two stage fusion method was used to extract silica and alumina form fly ash, then the blend was synthesized by mixing the extractants with $Na_2Al_2O_4$ and NaOH followed by gelification, aging and crystallization, the flow sheet diagram for the preparation procedure is illustrated in Fig. 2, the initial characterizations of the fly ash and the prepared zeolite are explained elsewhere [30,32].

2.3. Physical properties measurements

The prepared zeolite was subjected to laboratory measurements to determine its bulk density (ρ_d), porosity (ε), and particle size distribution. The bulk density and porosity measurements carried out in triplicate samples and tested according the ASTM annual book [33]. The particle size distribution was quantified using SALD 2001, Shinadzu, Japan laser diffraction particles size analyzer. The mean grain size D_{50} was evaluated and the coefficient of uniformity was determined using the following formula:

$$C_u = \frac{D_{60}}{D_{10}} \quad (1)$$

where D_x is the diameter particle having x percent fines.

2.4. Determination of cation exchange capacity (CEC)

To determine the cation exchange capacity of the prepared material, the zeolite samples were initially dispersed in 1.0 M sodium acetate trihydrate solution for 24 h, washed five times with distilled water (1 l/wash), filtered, and dispersed in ethanol for 24 h. Then, samples were filtered and dried for 24 h at 105 °C. A 50.0 ml

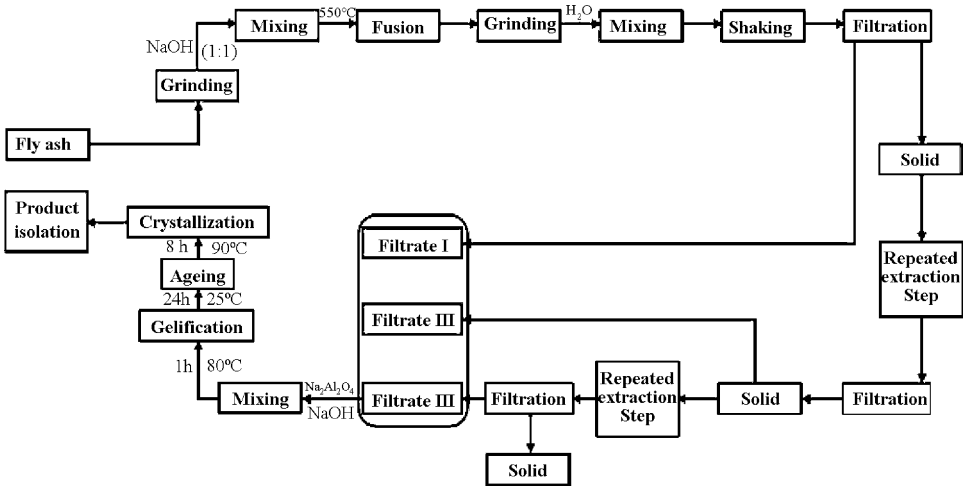

Fig. 2. Flow sheet diagram for the preparation of zeolite Na A-X blend.

ammonium acetate solution was mixed with 5.0 g zeolite and kept at ambient temperature of approximately 24 °C in a shaking water bath for 48 h. The supernatant was filtered and diluted to 100 ml with deionized water and the concentration of exchangeable Na^+ ions was determined using flame photometry.

2.5. Batch experiment

Batch sorption behavior of Cs ions on the synthetic zeolite Na A-X blend was conducted by immersing 0.1 g zeolite/100 ml of liquid phase. Then the samples were placed into centrifuge tube in triplicate and were shaken under constant vigorous shaking at ambient temperature. The suitability of the geochemical conditions was preliminary examined by varying the initial pH from 2 to 9. The transient behavior of the batch sorption was studied by withdrawing and centrifuging samples at different time intervals. The clear liquid phases obtained were measured by atomic absorption spectrophotometer (buck scientific, VGP 210). The amount of Cs ions sorbed onto the synthetic zeolite Na A-X blend at any time, q_t (mg/g) and the distribution coefficient K_d (ml/g) were calculated using the following equations:

$$q_t = (C_0 - C_t)\left(\frac{V}{m}\right) \tag{2}$$

$$K_d = \left(\frac{C_0 - C_e}{C_e}\right)\left(\frac{V}{m}\right) \times 10^3 \tag{3}$$

where C_0 and C_e are the initial and equilibrium concentration of Cs in the liquid phase (mg/l), V the volume (l) and m is the weight of the zeolite (g).

To determine the maximum sorption level of Cs onto the prepared material, batch experiment was carried out by immersing the zeolite Na A-X blend samples in a 10 g/l liquid phase under constant vigorous shaking at ambient temperature.

2.6. Column experiment

Column experiment was utilized to study the transport phenomena under saturated conditions. The synthetic zeolite Na A-X was placed under the liquid phase and maintained saturated through the experiment. The synthetic groundwater was initially permeated through the column to ensure that steady state condition was achieved before introducing the ion solution and to establish the outflow conditions at the outlet. To maintain a constant velocity stimulate to that exist under disposal conditions, the average linear velocity in the proposed backfill was obtained from the following equation:

$$v = \frac{\text{rate of water pentration into the facility}}{\varepsilon \times \text{effective cross-section}} \tag{4}$$

The velocity was controlled by controlling the quantity of discharged water per unit time. The discharge linear velocity used in the experiments was around 0.025 cm/h. The Cs concentration was measured using atomic absorption spectrophotometer. The experiment was conducted at ambient temperature of approximately 24 °C. The column length (L) and inner diameter (D) are 30 and 4.5 cm, respectively.

To determine the hydrodynamic dispersion coefficient in laboratory, the result of the column studies were reported in terms of effluent pore volume variable (U), which is defined as

$$U = \frac{\text{total discharged over a period of time}}{\text{volume of one pore volume}} = \frac{v\varepsilon At}{AL\varepsilon} = \frac{vt}{\varepsilon}$$

Then Brigham method [35] was adopted to determine the value of the hydrodynamic dispersion. In this method, Ogata–Banks solution [34] for transient concentration distribution for a non-reactive solute in saturated, homogenous, isotropic porous medium under one-dimensional steady-state uniform flow given by: $C/C_0 = 1/2[erf((L - v_f t)/(2\sqrt{D_L t}))]$ was rearranged in terms of the effluent pore volume (U) to yield

$$\frac{C}{C_0} = \frac{1}{2}\left[erfc\left(\frac{1-U}{2(UD_L/v_f L)^{1/2}}\right)\right]$$

Brigham recommended to plot the effluent relative concentration, C/C_0 as a function of $(U-1)/\sqrt{U}$ on linear probability scale. If the measured experimental data were presented as straight line then the hydrodynamic dispersion coefficient could be calculated using the following equation:

$$D_L = \frac{vL}{8}\left(\left.\frac{U-1}{\sqrt{U}}\right|_{0.84} - \left.\frac{U-1}{\sqrt{U}}\right|_{0.16}\right)^2 \tag{5}$$

3. Results and discussion

3.1. Results of the experimental investigations

The physical properties of the prepared zeolite are summarized in Table 2. These properties include: porosity (ε), bulk density (ρ_d), the mean grain size (D_{50}), and diameters of the zeolite particles for which 60% and 10% of the particles are finer (D_{60} and D_{10}).

The quantification of the particle size distribution shows that 50% of particles have a diameter smaller than (0.38) mm (D_{50}). The coefficient of uniformity C_u is found to be 1.6 that indicates that the prepared zeolite have a uniform particle size distribution that will reduce the probability of clogging failure [36].

The result of the cation exchange capacity experiment indicates that the prepared zeolite has a high-cation exchange capacity of 4.62 mequiv./g. The maximum sorption level of Cs was found to be 183.5 mg/g, where the calculation of the sorption capacity, determined form the equilibrium isotherm [30], was found to be 150.15 mg/g. The values calculated from the equilibrium isotherms is lower than that deduced form the maximum sorption capacity experiment, this might be attributed to the intensive conditions of high-initial Cs ion concentration under which the maximum sorption level was measured. To assess the cation exchange properties of the prepared material for the retention of Cs ions, the value of the sorption capacity was compared with that of other sorbents found in the literature. Table 3 shows that comparison, it can be concluded that zeolite Na A-X blend exhibits fairly high-sorption capacity towards Cs ions.

The pH of groundwater typically range from about 6.0 to 8.5 depending on the type of soil and rock that react with ground water, if the groundwater transport in coal or shale bedrock it can have pH lower than 4.0 because it has reacted with iorn sulfide minerals [45]. To check preliminary the suitability of the geochemical conditions, the retention of Cs ions onto the prepared zeolite Na A-X blend was studied at different pH ranging from 2 to 9. From the tabulated values of the distribution coefficient K_d versus pH, Table 4, it is clearly shown that the distribution coefficient K_d increases with

Table 2
Physical properties of the prepared zeolite.

Properties	Value
Porosity (ε)	0.6
Bulk density (ρ_d) (g/cm^3)	0.8
Mean grain size, D_{50} (mm)	0.38
D_{10} (mm)	0.25
D_{60} (mm)	0.4

Table 3
Comparison of cesium sorption capacities for various sorbents.

Sorbent	Sorption capacity (mg/g)	Ref.
Zeolite-A	207.47	[37]
Potassium-depleted phlogopite	167.45	[38]
A-X zeolite blend	150.15	Present work
Hydrous titanium oxide	126.92	[39]
Bentonite mineral	74.42	[40]
Nickel ferrocyanide based composite	66.45	[41]
Copper hexacyano-ferrate/polymer/silica composite	19.94	[42]
Red clay	4.91	[43]
Hydrous silicon dioxide	3.59	[44]

Table 4
Effect of pH and initial concentration on the distribution coefficient.

pH	K_d (ml/g)
2	220.0
3	233.3
4	428.5
5	562.5
6	1272.7
7	1500.0
8	1850.0
9	1860.0

increasing pH. This effect of pH on the retention ability of zeolite is stipulated by the fact that this material, as well as other aluminum silicates, are multifunctional sub-acid ionites [46,47]. Therefore, in the acid environment the exchange of different cations on the sorbent also involves competing hydrogen ions. The examination of the data revealed that two trends could be recognized. At low-pH values, K_d increases rapidly with increasing pH. While at pH higher than 6, K_d have a high and fairly constant values. This indicates that material will show a reasonbly retention performance at the studied mean value of the groundwater pH at Inshas site.

Fig. 3(a) shows the plot of the amount sorbed of Cs ions from liquid phase onto synthesized zeolite Na A-X blend, at initial Cs concentration of 50 mg/l and at ambient temperature, as a function of contact time. The figure shows a higher initial rate of sorption within the first 30 min followed by a slower subsequent sorption rate till reaching equilibrium.

To understand the nature of the sorption mechanism, the transient behavior of the batch sorption process of Cs ions was analyzed using the linear form of Lagergren, Ho and Mckay, and Morris–Weber models [48–50] using excel spreadsheet (Table 5). During the analysis of the experimental data using Lagergren model [48], it was observed form the examination of the plot of $\log(q_e - q_t)$ versus time (Fig. 4(a)) that the data are well represented by this model for the first 30 min. The result of the Lagergren model shows a respectively low-correlation coefficients (R^2). A considerable deviation between the experimental and calculated q_e values occurred (experimental q_e = 38.7 mg/g), confirms that it is not appropriate to use Lagergren kinetic model to represent the sorption kinetics of the Cs ions on the synthetic zeolite Na A-X blend for the entire sorption period. Further analysis of the experimental

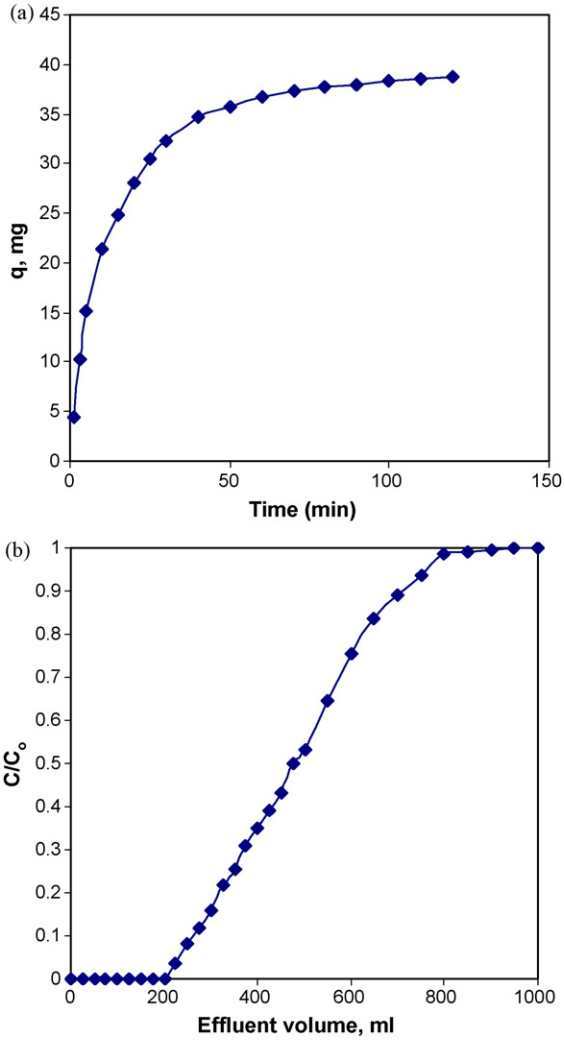

Fig. 3. (a) Effect of contact time on the sorption of Cs onto zeolite; (b) breakthrough curve of Cs onto zeolite.

data using the linear form of Ho and Mckay model indicates that the correlation coefficient (R^2), has extremely high value (>0.99), and the theoretical q_e value agree with the experimental value (Table 5 and Fig. 4(b)). These results suggest that the sorption process could be presented using this model, so the sorption process is chemisorption process [49]. To interpret the experimental data form the mechanistic point of view, the steps involved during the sorption process should be identified. In theory, the plot of q_t versus $\sqrt{t}$ is given by multiple regions representing different mechanisms of the sorption process [51]. The examination of the plot of q_t versus $\sqrt{t}$ could be divided into two regions indicating the occurrence of two mechanisms during the sorption of Cs onto synthetic zeolite Na A-X blend (Fig. 4(c)). The fit of the experimental data in the first region pass through the origin and the rate constant for the particle diffusion was calculated from the slope of Fig. 4(d).

Table 5
Result of the kinetic studies.

Model	Equation	R^2	Model parameter
Lagergren	$\log(q_e - q_t) = \log q_e - \frac{k_1}{2.303}t$	0.9809	q_e = 29.4 mg/g, k_1 = 0.0458 min^{-1}
Ho and Mckay	$\frac{t}{q_t} = \frac{1}{h} + \frac{1}{q_e}t$	0.9998	q_e = 39.8 mg/g, h = 4.599 mg/(g min), k_2 = 0.0026 g/(mg min)
Morris–Weber	$q_t = K_{ad}\sqrt{t}$	0.9984	K_{ad} = 6.294 mg/(g min$^{0.5}$)

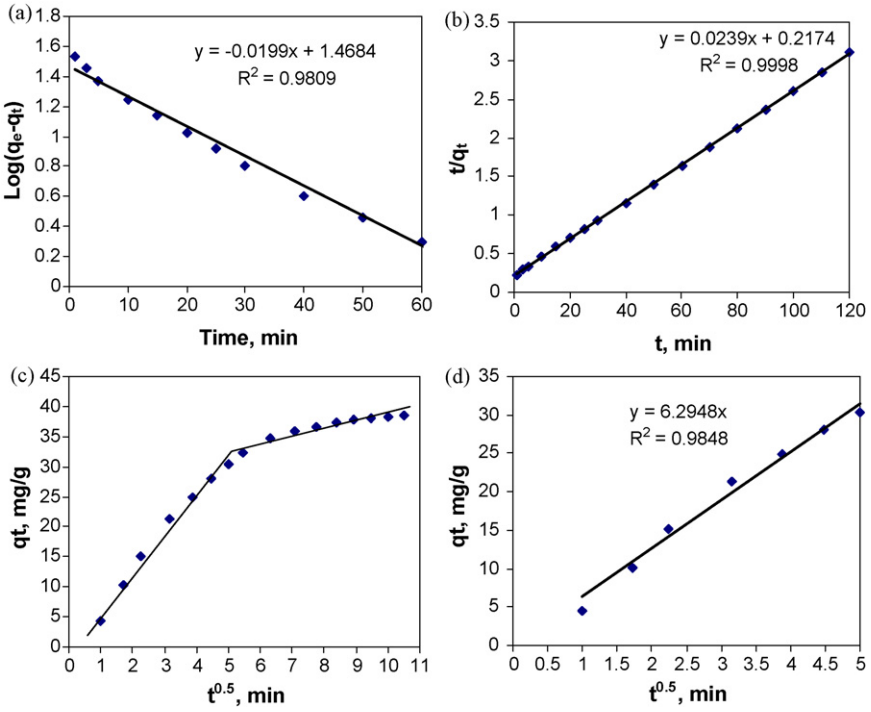

Fig. 4. (a–d) Comparison of kinetic sorption models of Cs onto synthetic zeolite Na A-X blend.

Fixed bed column sorption experiments were carried out to study the dispersional behavior of cesium on synthetic zeolite Na A-X blend. The shape of the breakthrough curve and the time for the breakthrough appearance are the predominant factors for determining the dynamic response of the sorption column. In this concern, the loading behavior of Cs ions sorbed onto zeolite Na A-X from synthetic ground water solution in a fixed bed are shown by breakthrough curve (Fig. 3(b)) that are expressed in terms of normalized concentration, defined as the ratio of effluent ion concentration to its inlet concentration (C_t/C_0), as a function of effluent volume for a given bed height. From Fig. 3(b), it is clearly shown that the breakthrough curve displayed the classical 'S'-shaped curve. It was observed in the test that the mean contaminant velocity (v_c) was always greater than the linear average pore water velocity (v). The examination of the plot of effluent relative concentration, C/C_0 versus $(U-1)/\sqrt{U}$ on linear probability scale, was illustrated as a straight line. The dispersion coefficient was calculated using Eq. (6) and found to be 0.129 m^2/yr.

3.2. Long-term performance assessment of synthetic zeolite NaA-X blend

The potential impact to soil and groundwater contamination from the disposed radioactive waste over long period of time represents a common environmental concern. This concern is addressed by performing environmental risk assessment for potential leaks of dissolved radionuclides to the hosted environment. The aim of this section is to assess the long-term performance of the synthetic zeolite Na A-X blend as a backfill material in terms of radionuclide containments. In this respect, the potential leak of Cs from bare waste form is assessed. The assessment methodology is illustrated in Fig. 5(a).

3.2.1. Description of the studied system

Fig. 5(b) presents a schematic drawing of the studied system, in which the waste packages and the backfill material are disposed

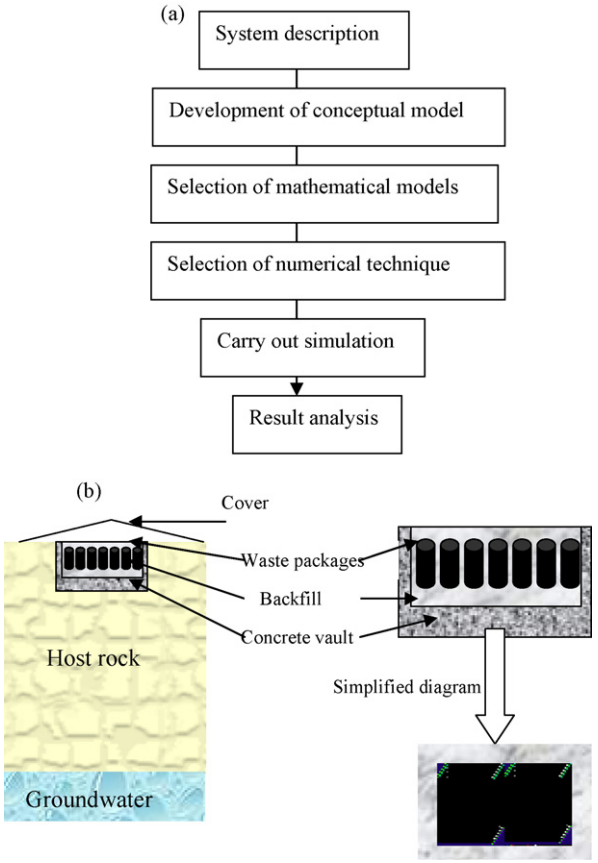

Fig. 5. (a) Performance assessment steps. (b) Schematic diagram of near surface disposal.

Table 6
Features, events, and processes that lead to the failure of disposal components.

Component	FEP	FEP n
Cover	Wind and rain erosion	2.3.12
	Cracking and desiccations	2.1.05
Vault	Internal changes (i.e. crystallization, alkyl aggregates reactions)	3.2.01
	Chemical reaction with ground water and hosted environment	2.1.09
	Thermal stresses (i.e. resaturation–desaturation, freeze–thaw cycles)	2.1.11
	Corrosion of reinforcement	2.1.06
Containers	Subsidence as a results of compression	2.1.07
	Chemical reaction with the pore water	2.1.03

in a shallow reinforced concrete vault. The facility is placed on an excavation of a foundation and covered with topsoil cover. After the closure of the disposal vault, the engineered barriers will prevent any release of the radionuclides during the lifetime of these barriers. The degradation of the engineered barriers may proceed through different possible feature, event and processes (FEP). A list of these FEPs was adopted from the ISAM FEPs [52] list as indicated in Table 6.

3.2.2. Development of conceptual model

Generally, a conceptual model describes with words and diagrams the key processes that occur within the studied system (or have a reasonable likelihood of occurring). These models can be formulated at varying levels of complexity and realism to abstract the reality [53]. The developed conceptual model forms the basis for the selection of mathematical models, which in turn govern the selection and creation of numerical models and computer codes. Generally, the immobilized waste is encased in a package to prevent direct contact of the waste with the water so that no leaching occurs during the lifetime of the package. However, this concept of delay in not considered in this work to assess the performance of the backfill material under release from bare waste form as a conservative scenario. The radionuclides will be leached out from bare immobilized waste form then migrate through the porous backfill material. The key processes considered in this study are illustrated in Fig. 6.

3.2.3. Selection of mathematical models

To obtain the radionuclide release rate and concentration profile through the proposed backfill material due to leach flux from the waste form, the convolution approach was adopted. This approach for estimating groundwater concentrations, conceptually described by Lee [54], simulates a system response from a unit inventory release through each disposal barrier. It then uses the results with principles of superposition to estimate groundwater concentrations for a specific constituent inventory distribution. This approach is useful in estimating groundwater concentrations at specific locations and can be a preferred alternative when there are more combinations of inventory distributions and parameter sets. In this study, the radionuclide leach flux from a bare waste form is first predicted independently in the waste module. Then by making the assumption of linearity, the unit release responses from each individual source area in the waste module is combined or superimposed with the backfill migration module.

Waste module, there are several models to study the leaching behavior of radionuclides from cementious waste forms. A leaching model based on the internal diffusion controlled kinetics has been selected to assess the transfer of radionuclides from the waste form into the surrounding pore water of the backfill material. The rate of change of radionuclide concentration in the waste form is given by the mass transport equation:

$$\frac{\partial C_w}{\partial t} = \frac{D_w}{Rd}\left[\frac{\partial^2 C_w}{\partial x^2} + \frac{\partial^2 C_w}{\partial y^2}\right] - \lambda C_w \tag{6}$$

where x and y are the spatial coordinate in flow direction and perpendicular direction, respectively (cm), t the time (s), C_w the cesium concentration in the waste form (Bq/ml), D_w the cesium diffusivity in the waste form (cm^2/s), λ the cesium decay constant, and Rd is the retardation coefficient in the waste defined by

$$Rd = \left(1 + \frac{K_d \rho_d}{\varepsilon}\right) \tag{7}$$

where ε is the effective porosity of the zeolite, ρ_d the bulk density (g/cm^3) and K_d is the distribution coefficient (cm^3/g).

Assuming that, the radionuclides are uniformly dispersed through the waste form on the macroscopic view, and that the mass transfer external to the waste form is faster than the internal transfer in the matrix, the initial and boundary conditions can be written as follows:

$$C_w(x, y, 0) = C_0, \quad C_w(a, y, t) = 0, \quad C_w(x, b, t) = 0 \tag{8}$$

where a and b are the dimensions of the waste matrix in the x and y directions.

Also, the flux of radionuclide release from the waste form can be calculated using the following equation:

$$Rate = -\int_A D\frac{\partial C_w}{\partial x}\bigg|_{x=a} dA \tag{9}$$

where A is the area of the interface.

Backfill module. Radionuclides migration through the backfill material is governed by advection, dispersion, retention,

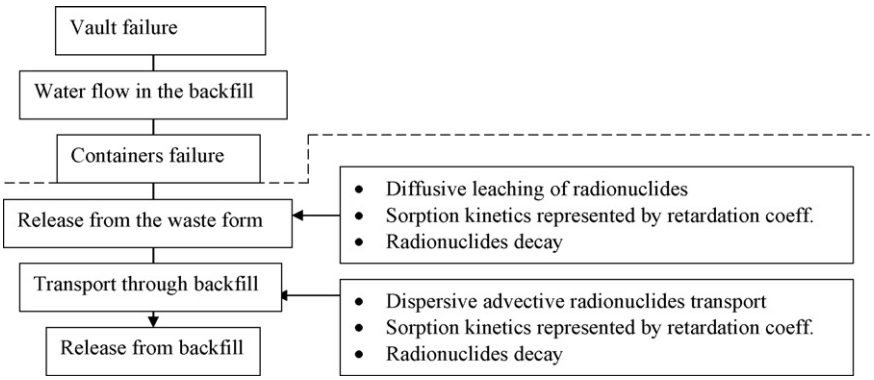

Fig. 6. Release pathway from the immobilized waste form.

and radionuclides decay. Advection represents the movement of radionuclides with the flow of the penetrated water and dispersion is the combination of molecular diffusion due to concentration gradient and hydrodynamic dispersion due to the deviation of the local water velocity from its average value. Retention represents interactions that take place between radionuclides and backfill materials, including reversible and irreversible chemical adsorption, physical adsorption, molecular diffusion to immobile water filtration, precipitation/dissolution, aggregation, and so on. The identification of all of the mechanisms that take place, however, is so far still to be worked out. Even if some potential mechanism is successfully identified and modeled precisely, the computation with that model requires a much greater database than that currently available (e.g. radiochemical speciation data, kinetic parameters corresponding to each interaction mechanism, geochemical equilibrium data, a complete mineralogical compositions of the material and also, local variation of theses parameters). Therefore, the basic retention mechanisms were not specifically distinguished in this study, but their total effects that retard the migration of cesium radionuclides were assumed to be empirically represented by the distribution coefficient, K_d obtained from the batch sorption experiment. The use of K_d in this study is based on the following assumptions; K_d is independent on the concentration of the cesium, each radionuclide migrates independently of the others, and each retention occurs instantaneously and reversibly.

Based on the above assumptions the two-dimensional migration equation could be derived from the mass balance over a unit volume of the backfill as follows:

$$\frac{\partial C_b}{\partial t} = D_{xx}\frac{\partial^2 C_b}{\partial x^2} + D_{yy}\frac{\partial^2 C_b}{\partial y^2} - v_x\frac{\partial C_b}{\partial x} - v_y\frac{\partial C_b}{\partial y} - \lambda C_b \quad (10)$$

where D_{xx} and D_{yy} are the hydrodynamic dispersion coefficient along the direction of flow and perpendicular on it, respectively.

Assuming that, the backfill was initially contain no radionuclides then the radionuclides at the bare waste form are allowed to migrate through the inner edge of the backfill. The initial and boundary conditions are given as follows:

$$C_b(x, y, 0) = 0 \quad (11)$$

$$C_b(0, y, t) = 1, \quad C_b(x, 0, t) = 0, \quad C_b(x, b, t) = 0, \quad C_b(a, y, t) = 0 \quad (12)$$

The concentration of radionuclides (Bq/ml) in pore water of backfill for instantaneous release of unit radioactivity (1 Bq) into the backfill, C_b was obtained by solving Eq. (9) (the governing equa-

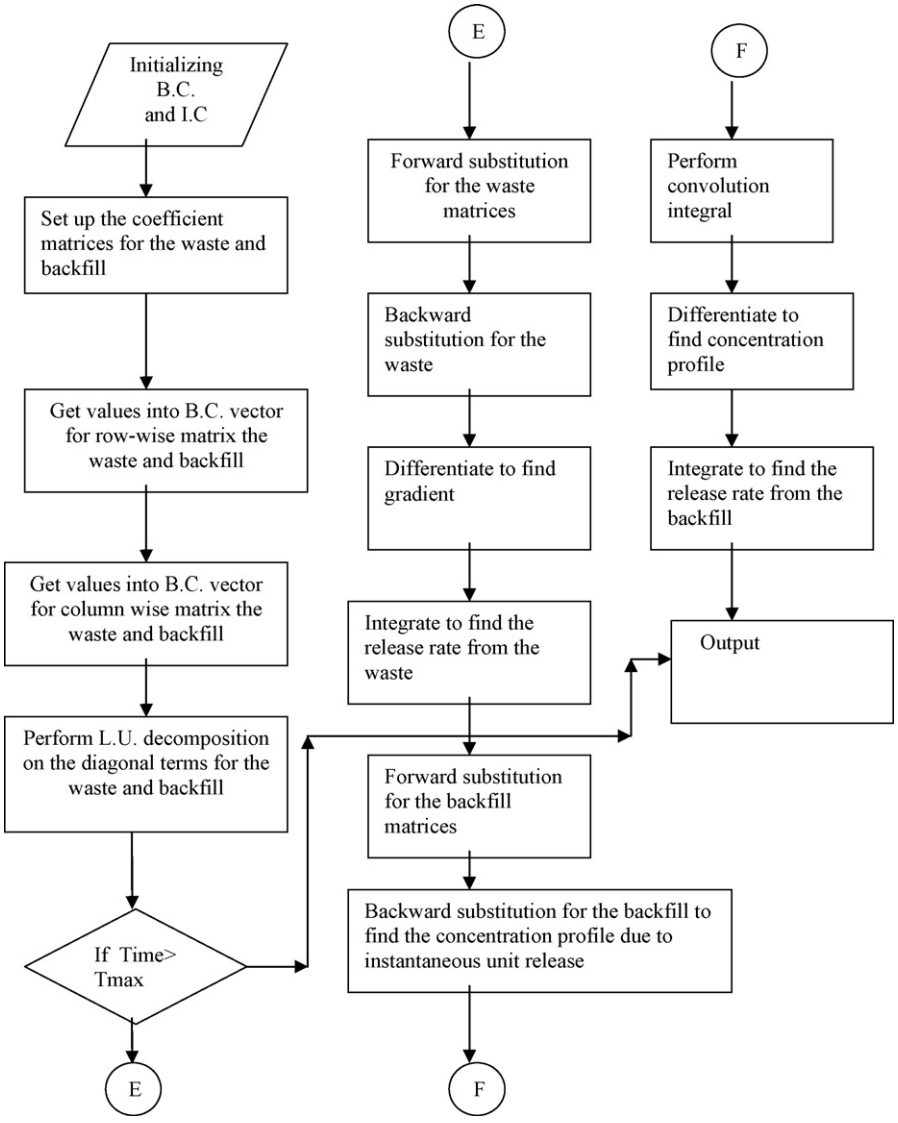

Fig. 7. Designed program flowchart.

tion in backfill), then the concentration of radionuclides in the pore water of the backfill material, C (Bq/ml) due to leach flux from the waste form was obtained by the principle of superposition of the radionuclide flux obtained from the waste module and the radionuclides concentration in the pore waste of backfill for instantaneous radioactivity unit release into the backfill using the of the following convolution integral:

$$C(x, y, t) = \int_{\tau=0}^{t} Rate(t-\tau) C_b(x, y, \tau)\, d\tau \quad (13)$$

Then release rate of radionuclides from the combined barriers (bare waste form and backfill) can be calculated using

$$Rate = -\int_A D \frac{\partial C_w}{\partial x}\bigg|_{x=a} dA \quad (14)$$

3.2.4. Selection and development of solution technique

Extensive research has been and is being carried out on the numerical aspects of simulating contaminant transport. Several researches have explored alternative numerical techniques for solving partial differential equations that describe the contaminant transport. The objective of these studies include obtaining more stable numerical algorithm, speeding up the calculations, minimizing mass balance errors, and achieving more accurate solutions for different initial and boundary conditions. The aim of this section is to present the development of the numerical tool that has been used to quantitatively predict Cs migration through the backfill. This tool solves the governing equations (6–14) by means of finite difference technique and using a scheme based on the alternative direction implicit (ADI) formulation.

ADI formulation was introduced by Peaceman and Rachford [55] for solving equations arising from finite difference discretization of partial differential equations. ADI has proved valuable performance in the approximation of the solutions of parabolic and elliptic differential equations in two and three dimensions. This formulation embodies a powerful concept of operator splitting or time splitting. The basic idea is to divide each time step into two steps of size $\Delta t/2$, in each sub-step a different dimension is treated implicitly. The advantage of this method is that each sub-step requires only the solution of tri-diagonal system [56]. Peaceman–Rachford ADI algorithm for the linear system $Ax = b$, is given as follows:

For $k = 0, 1, \ldots$ until convergence

(1) solve$(U + \rho I)x_{k+0.5} = (\rho I - V)u_k + b$
(2) solve$(V + \rho I)x_{k+1} = (\rho I - U)u_{k+0.5} + b$

where U and V are discretized differential operations and are related to horizontal and vertical directions, respectively and ρ is a positive acceleration parameter.

The first step in the development of the numerical tool either for the waste or backfill module is the discretization, at which partial differential equation is transformed into algebraic one. To develop the discrete equations for each module, the studied area is subdivided into a number of small elements by passing orthogonal lines through the region. Then implicit Crank–Nicalson scheme was applied to obtain the discrete form of Eqs. (5) and (9) followed by the application of ADI. Finally, the solution was obtained by solving the tri-diagonal matrices to yield values for concentrations at all nodes by lower–upper (LU) decomposition algorithm.

A computer program was developed and tested for personal computer under windows environment using Fortran language, the flowchart of the program is illustrated in Fig. 7. The examination of the numerical solution stability relative to some parameters allows the definition of the domain of applicability of a given numerical scheme. These parameters also allow the determination of the optimum grid and time step for a stable solution of the problem under consideration. Earlier studies demonstrates that the ADI scheme is second order accurate in time and space, and unconditionally stable when applied to the diffusion equation (the waste module) [56–58]. On the other hand, other studies indicate that the ADI scheme is conditionally sable for convection dominated problems (high-Pe number) [59] . In the studied cases, water velocity was very small to simulate possible disposal conditions so Pe number has a very small value.

3.2.5. Carry out simulation

In order to evaluate the long-term performance of the proposed material, the leaching of Cs radionuclides from bare waste form through zeolite Na A-X blend backfill was simulated. The relative concentration profile of Cs radionuclides through the proposed backfill material after 300 years is shown in Fig. 8(a), at which the concentration profile reduced significantly after 10 cm from the waste. Bentonite and crushed rock backfill is commonly proposed for nuclear repository, this backfill was studied as a comparative material. The general, physical and transport parameters used in the conducting the simulations are listed in Table 7 [60]. The release rate from the waste form, bentonite and crushed rock mixture and the prepared zeolite as a function of time is shown in Fig. 8(b). By comparing the performance of the zeolite to that of bentonite mixture, it was found that, for the studied inventory, the release rate from the waste module will be 8.6 Bq/yr, the utilization of the ben-

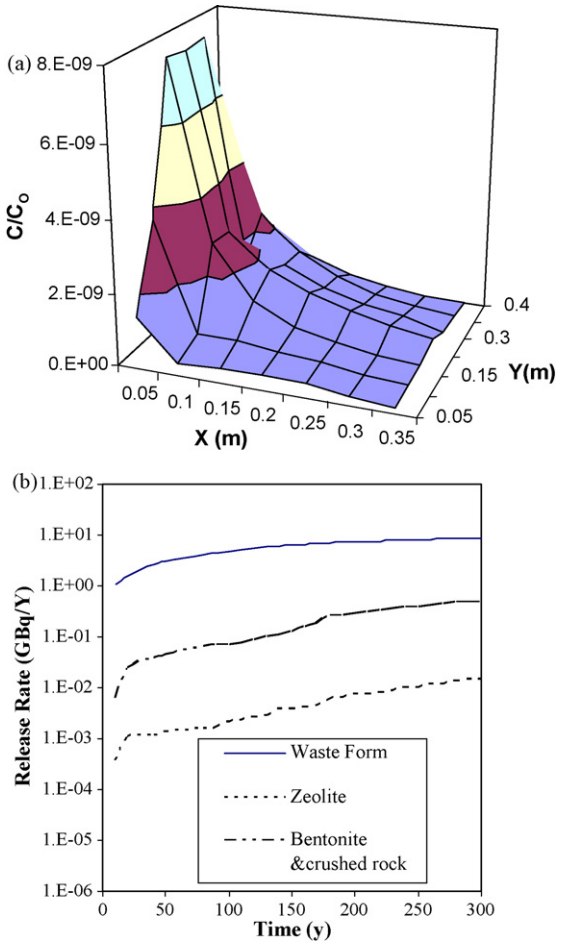

Fig. 8. (a) Relative concentration profile; (b) release rate form the waste, zeolite, and bentonite.

Table 7
Input parameters for the performance study.

Parameters description	Value
Time scale of the study	300 yr
Initial concentration (Bq/l)	6.6×10^{10}
Half life of Cs (yr)	30.2
Waste form	
Dimensions	$4\,m \times 4\,m \times 3\,m$
Porosity	0.15
Density (g/cm^3)	1.3
Cs K_d (ml/g)	2.0
Diffusion coefficient (m^2/yr)	3×10^{-6}
Bentonite and crushed rock mixture	
Porosity	0.15
Density (g/cm^3)	1.4
K_d (ml/g)	20
Diffusion (m^2/yr)	0.127

tonite and crushed rock backfill will reduce the release by 16 order, where using the zeolite will reduce the release by 10^3 order. This could be attributed to the high sorptivity of zeolite for the studied radionuclide.

4. Conclusion

The technical feasibility of using zeolite NaA-X was examined by evaluating the physical, and chemical properties of the zeolite, then the long-term behavior of the material was assessed using a computer model. The specific conclusions pertaining to the results presented herein can be drawn as follows:

(1) The examination of the particle size distribution and the coefficient of uniformity indicates that the prepared zeolite has a uniform particle size distribution that will reduce the probability of clogging.
(2) The geochemical condition at the disposal site are favorable conditions for the uptake of Cs since the pH of the groundwater was found to be 6.5 and high-distribution coefficients was observed at pH range 6–8.
(3) By analyzing the experimental batch sorption data to different kinetic models, an insight was gained on the predominant mechanism that controls the sorption behavior. It was found that this sorption process is a chemisorption process and particle diffusion is the dominant sorption mechanism.
(4) By fitting the column experimental data to Brigham method the hydrodynamic dispersion coefficient was found to be $0.129\,m^2$/yr.
(5) Numerical model was developed to solve the governing equations by mean of finite difference technique using ADI scheme, literature studies found that the result of the simulation will be unconditionally stable for the diffusion equation and conditionally stable by controlling Pe. The numerical stability of the model was checked by evaluating Pe number.
(6) The comparison between the performance of the synthetic zeolite Na A-X blend to that of bentonite and crushed rock mixture in terms of radionuclide containment. It was found that the prepared zeolite has significantly reduced the release form the waste form.
(7) The conducted work showed that the zeolite have proven a good behavior in the containment of the studied radionuclide, further investigation will be carried out to investigate the mechanical behavior of the prepared material.

References

[1] Planning and operation of low level waste disposal facilities, in: Proc. Symp. Vienna, 1996, IAEA, Vienna, 1997.
[2] International Atomic Energy Agency, Performance of Engineered Barriers in Deep Geological Repositories, Technical Reports Series No. 342, Vienna, 1992.
[3] International Atomic Energy Agency, Review of Available Options for Low level Radioactive Waste Disposal, IAEA-TECDOC-661, IAEA, Vienna, 1992.
[4] International Atomic Energy Agency, Report on Radioactive Waste Disposal, Technical Reports Series No. 349, IAEA, Vienna, 1993.
[5] United States Environmental Protection Agency, International Workshop on the Use of Backfill in Nuclear Waste Repositories, Carlsbad, New Mexico, USA, May 1998, R&D Technical Report, 1998, p. 178.
[6] United States Department of Energy, Conceptual Design Report: Alternative Concepts for Low-Level Radioactive Waste Disposal, DOE/LLW-60T, 1987.
[7] B. Allard, L.O. Hoglud, K. Skagius, Adsorption of Radionuclides in Concrete, Rep. Sfr-91-02, SKB, Stockholm, 1991.
[8] E. Hooft, Working with local partners: approach to the disposal of short-lived low-level radioactive waste, in: Proceedings of TOPSEAL'99, 1999.
[9] R.J. Mitchell, Stability of cemented tailings mine backfill, in: Balasubramaniam, et al. (Eds.), Proceedings Computer and Physical Modeling in Geotechnical Engineering, A.A. Balkema, Rotterdam, 1989, pp. 501–507.
[10] R.N. Yong, P. Boonsinsuk, G. Wong, Formulation of backfill material for a nuclear fuel waste disposal vault, Canadian Geotechnology Journal 23 (1996) 216–228.
[11] J.J.K. Daemen, C. Ran, Bentonite as a Waste Isolation Pilot Plant Shaft Sealing Material. Sandia National Laboratories, Albuquerque, Contractor Report SAND96-1968, 1996.
[12] D.E. Daniel, in: D.E. Daniel (Ed.), Clay Liners in Geotechnical Practice for Waste Disposal, Chapman and Hall, London, 1993, pp. 137–163.
[13] R.K. Rowe, R.M. Quigley, J.R. Booker, Clayey Barrier Systems for Waste Disposal Facilities, E&FN Spon, London, 1995.
[14] N.H. Akgu, J.K. Daemen, Design implications of analytical and laboratory studies of permanent abandonment plugs, Canadian Geotechnology Journal 36 (1) (1999) 21–38.
[15] L. Borgesson, M. Chijimatsu, T. Fujita, T.S. Nguyen, J. Rutqvist, L. Jing, T–H–M characterization of a bentonite-based buffer materials by laboratory tests and numerical back analysis, International Journal of Rock Mechanics and Mining Sciences 38 (2001) 95–104.
[16] H. Komine, Simplified evaluation on hydraulic conductivities of sand–bentonite mixture backfill, Applied Clay Science 26 (2004) 13–19.
[17] H. Komine, N. Ogata, Experimental study on swelling characteristics of compacted bentonite, Canadian Geotechnology Journal 31 (1994) 478–490.
[18] H.S. Radhakrishna, H.T. Chan, Thermal and physical properties of candidate buffer–backfill materials for nuclear fuel waste disposal vault, Canadian Geotechnology Journal 26 (1989) 629–639.
[19] K.A. Bout, M.M. Cowper, T.G. Heath, H. Sato, T. Shibutani, M. Yui, Toward and understanding of the sorption of U(VI) and Se(IV) on sodium bentonite, Journal of Contaminant Hydrology 35 (1998) 141–150.
[20] A. Muurinen, J. Lehikoinen, Pore water chemistry in compact bentonite, Engineering Geology 54 (1999) 207–214.
[21] S.C. Tsai, S. Ouyang, C.N. Hsu, Sorption and diffusion behavior of Cs and Sr on Jih–Hsing bentonite, Applied Radiation and Isotope 54 (2001) 209–215.
[22] Y.-L. Jan, S.-C. Tsai, Y.-Y. Wei, N.-C. Tung, C.-C. Wei, C.-N. Hsu, Coupled mechanics, hydraulics and sorption properties of mixtures to evaluate buffer/backfill materials, Physics and Chemistry of the Earth 32 (2007) 789–794.
[23] M. Othman, C. Benson, E. Chamberlain, T. Zimmie, Laboratory testing to evaluate changes in hydraulic conductivity caused by freeze–thaw: state-of-the-art, Hydraulic Conductivity and Waste Contaminant Transport in Soils, ASTM, STP 1142 (1994) 227–254.
[24] C.H. Benson, A.M. Othman, Hydraulic conductivity of compacted clay frozen in situ, Journal of Geotechnical Engineering ASCE 119 (2) (1993) 276–294.
[25] C.H. Benson, T.H. Abichou, M.A. Olson, P.J. Bosscher, Winter effects on hydraulic conductivity of compacted clay, Journal of Geotechnical Engineering 121 (1) (1995) 69–79.
[26] W.S. Abdullah, K.A. Alshibli, M.S. Al-Zou'bi, Influence of pore water chemistry on the swelling behavior of compacted clays, Applied Clay Science 15 (1999) 447–462.
[27] E.J. Chamberlain, I. Iskender, S.E. Hunsiker, Effect of freeze–thaw on the permeability and macrostructure of soils, in: Proceedings, International Symposium on Frozen Soil Impacts on Agricultural, Range, and Forest Lands, March 21–22, Spokane, WA, 1990, pp. 145–155.
[28] A. Kaya, S. Durukan, Utilization of bentonite-embedded zeolite as clay liner, Applied Clay Science 25 (2004) 83–91.
[29] K. Kayabalı, Engineering aspects of a novel landfill material: bentonite amended natural zeolite, Engineering Geology 46 (1997) 105–114.
[30] H.A. Ibrahium, A.M. El-Kamash, M. Hanafy, N.M. Abdel Monem, Examination of the use of synthetics zeolite Na-AX blends as backfill material in a radioactive waste disposal facility, Chemical Engineering Journal 144 (1) (2008) 67–74.
[31] A.M. El Kamash, M.R. El Naggar, M.I. El Dessouky, Immobilization of cesium and strontium radionuclides in zeolite cement blends, Journal of Hazardous Materials 136 (2006) 310–316.
[32] M.R. El-Naggar, Chemical studies on preparation and characterization of zeolite material from fly ash for treatment of radioactive liquid wastes, PhD thesis, Faculty of Science, Zagazig University, 2008.

[33] ASTM, Soil and Rock. Construction. Annual Book of ASTM Standard, Section 4, Vol. 04.08, ASTM, Philadelphia.
[34] Ogata, R.B. Banks, A solution of the differential equation of the longitudinal dispersion in porous media, Fluid Movement in Earth Materials, Geological Survey Professional Paper 441, 1961.
[35] C.W. Fetter, Contaminant Hydrology, Macmillan Publishing Company, 1993, pp. 66–67.
[36] R.O. Abdel Rahman, Preliminary evaluation of the technical feasibility of using different soils in waste disposal cover system, in press.
[37] A.M. El-Kamash, Journal of Hazardous Materials 151 (2008) 432–445.
[38] Stout, et al., Journal of Applied Clay Science 31 (2006) 306–313.
[39] Metwally, et al., Journal of Radiochimica Acta 95 (2007) 409–416.
[40] G. Atun, N. Bodur, Journal of Radioanalytical and Nuclear Chemistry 253 (2) (2002) 275–279.
[41] J. Orchovska, P. Rajec, Journal of Radioanalytical and Nuclear Chemistry 242 (2) (1999) 387–390.
[42] S. Milonjic, I. Bispo, M. Fedoroff, C. Loos, C.V. Madjar, Journal of Radioanalytical and Nuclear Chemistry 252 (3) (2002) 497–501.
[43] T. Aküz, S. Aküz, A. Bassari, Journal of Inclusion Phenomena and Macrocyclic Chemistry 38 (2000) 337–344.
[44] P.N. Pathak, G.R. Choppin, Journal of Radioanalytical and Nuclear Chemistry 270 (2) (2006) 299–305.
[45] J.D. Hem, Study and Interpretation of the Chemical Characteristics of Natural Water, US Geological Survey, Water Supply Paper, Paper 2254, 1985, 263 p.
[46] A.Yu. Lonin, A.P. Krasnopyorova, Influence of different factors on sorption of 90Sr by natural and synthetic zeolite, Problems of Atomic Science and Technology, 2005, No. 6. *Series*: Nuclear Physics Investigations (45), 2005, pp. 130–132.
[47] T. Tamura, D.G. Jacobs, Structural implications in cesium sorption, Health Physics 2 (1960) 391–398.
[48] Y.S. Ho, G. McKay, A kinetics study of dye sorption by biosorbent waste product pith, Resources Conservation and Recycling 25 (1999) 171–193.
[49] G. McKay, Y.S. Ho, Pseudo-second order model for sorption processes, Process Biochemistry 34 (1999) 451–460.
[50] W.J. Weber, J.M. Morris, J. Sanit, Engineering Division of American Society of Engineers 89 (1963) 31–39.
[51] K.V. Kumar, H.S. Ramamurthi, S. Sivanisan, modeling the mechanism involved during the sorption of methylene blue onto fly ash, Journal of Colloid and Interface Science 284 (2005) 14–21.
[52] ISAM, Development of an Information System for Features, Events and Processes and Generic Scenarios for the Safety Assessment of Near Surface Radioactive Waste Disposal Facility ISAM/SWG/0298, 1999.
[53] Environment Agency, Guide to Practice for the Development of Conceptual Models and Selection and Application of Mathematical Models of Contaminant Transport Processes in the Subsurface, National Groundwater and Contaminated Land Center Report NC/99/38/2, 1999.
[54] T. Lee, Applied Mathematics in Hydrogeology, Lewis Publishers, Boca Raton, Florida, 1999.
[55] D. Peaceman, H. Rachford, The numerical solution of elliptic and parabolic differential equations, Journal of SIAM 3 (1955) 28–41.
[56] Y. Saad, Iterative Methods for Sparse Linear Systems, International Thomson Publishing, Boston, 1996.
[57] W. Dai, A generalized Peaceman–Rachford ADI scheme for solving two-dimensional parabolic differential equations, Journal of Scientific Computing 12 (4) (1997) 253–360.
[58] W. Press, S. Teukolsky, W. Vetterling, B. Flannery, Numerical recipes in Fortran 77 the art of scientific computing, in: Volume 1 Fortran Numerical Recipes, Cambridge University Press, 1993.
[59] S. Karaa, J. Zhang, High order ADI method for solving unsteady convection diffusion problems, Journal of Computational Physics 198 (2004) 1–9.
[60] A.M. El-Kamash, R.O. Mohamed, M.E. Nagy, M.Y. Khalil, Modeling and validation of radionuclides releases from an engineered disposal facility, International Journal of Waste Management and Environmental Restoration 22 (4) (2002) 373–393.